REPORT DOCUMENTATION PAGE

Form Approved
OMB No. 0704-0188

PLEASE DO NOT RETURN YOUR FORM TO THE ABOVE ADDRESS.

1. REPORT DATE *(DD-MM-YYYY)*	2. REPORT TYPE	3. DATES COVERED *(From - To)*
03092006	Final Report	01 February 2003 - 30 June 2006

4. TITLE AND SUBTITLE

Thermodynamic Descriptions of Ni Alloys Containing AL, CR, and RU: A Computational Thermodynamic Approach Coupled with Experiments

5a. CONTRACT NUMBER

5b. GRANT NUMBER

F49620-03-1-0083

5c. PROGRAM ELEMENT NUMBER

6. AUTHOR(S)

Dr. Y. Austin Chang

5d. PROJECT NUMBER

5e. TASK NUMBER

5f. WORK UNIT NUMBER

7. PERFORMING ORGANIZATION NAME(S) AND ADDRESS(ES)

Department of Materials Science & Engineering
University of Wisconsin
Madison WI

8. PERFORMING ORGANIZATION REPORT NUMBER

9. SPONSORING/MONITORING AGENCY NAME(S) AND ADDRESS(ES)

USAF/AFRL
AFOSR
875 North Randolph Street
Arlington VA 22203
Dr Jaimie Tiley/NA

10. SPONSOR/MONITOR'S ACRONYM(S)

AFOSR

11. SPONSOR/MONITOR'S REPORT NUMBER(S)

AFRL-SR-AR-TR-06-0381

12. DISTRIBUTION/AVAILABILITY STATEMENT

Distribution Statement A. Approved for public release; distribution is unlimited.

13. SUPPLEMENTARY NOTES

14. ABSTRACT

Shortly after initiating this program, we focused our effort to develop thermodynamic descriptions of ternary Ni-Cr-Ru and Ni-Al-Ru including the constituent binaries when needed using the traditional Calphad approach. In addition, we extended our effort to include the use of the Cluster/Site Approximation (CSA) to describe the fcc phases in the disordered and ordered states such as the prototype Cu-Ag-Au in 2003/2004 and then / ' in real ternary systems in 2004/2005. In the meantime, we began to explore the possibility of using CSA to calculate interphase boundary (IPB) energies of coherent interfaces such as those for / ' in prototype Cu-Au binary and then real binaries such as Ni-Al. The preliminary results on CSA-calculated prototype Cu-Ag-Au diagrams and IPB energies on prototype Cu-Au and Ni-Al were presented at the 2004 annual review meeting at Wintergreen, VA. We subsequently discussed with Dr. C. Hartley about our IPB energy effort and were encouraged to continue this research effort as part of our program.

15. SUBJECT TERMS

16. SECURITY CLASSIFICATION OF:			17. LIMITATION OF ABSTRACT	18. NUMBER OF PAGES	19a. NAME OF RESPONSIBLE PERSON
a. REPORT	b. ABSTRACT	c. THIS PAGE			19b. TELEPHONE NUMBER *(Include area code)*
U	U	U	UU	17	

THERMODYNMAIC DESCRIPTIONS OF NI ALLOYS CONTAINING AL, CR, AND RU: A COMPUTATIONAL THERMODYNAMIC APPROACH COUPLED WITH EXPERIMENTS

F49620-03-1-0083

Final Report

(9/3/06)

Y. Austin Chang
Department of Materials Science & Engineering
University of Wisconsin-Madison, WI

Abstract

Shortly after initiating this program, we focused our effort to develop thermodynamic descriptions of ternary Ni-Cr-Ru and Ni-Al-Ru including the constituent binaries when needed using the traditional Calphad approach. In addition, we extended our effort to include the use of the Cluster/Site Approximation (CSA) to describe the fcc phases in the disordered and ordered states such as the prototype Cu-Ag-Au in 2003/2004 and then γ/γ' in real ternary systems in 2004/2005. In the meantime, we began to explore the possibility of using CSA to calculate interphase boundary (IPB) energies of coherent interfaces such as those for γ/γ' in prototype Cu-Au binary and then real binaries such as Ni-Al. The preliminary results on CSA-calculated prototype Cu-Ag-Au diagrams and IPB energies on prototype Cu-Au and Ni-Al were presented at the 2004 annual review meeting at Wintergreen, VA. We subsequently discussed with Dr. C. Hartley about our IPB energy effort and were encouraged to continue this research effort as part of our program.

Developing a thermodynamic description of Ni-Al-Ru has been truly challenging using the limited and often-inconsistent experimental data reported in the literature. Obtaining a thermodynamic description for an alloy system is not purely a mathematical fit of the experimental data to a set of mathematical equations. Rather the obtained parameters must be physically reasonable in terms of the enthalpy and entropy quantities. We had every reason to believe that the phase equilibrium data reported in the literature could be in error. Nevertheless we tried our best to obtain a set of thermodynamic parameters for all the phases in this alloy system. Based on the calculated phase diagrams using the preliminarily obtained thermodynamic description, we identified a limited number of alloy compositions for investigation either to verify the calculation or more likely in this case to allow us to obtain an improved description! The experimental results indicate that this indeed is the case. An improved thermodynamic description of this technologically important ternary was then obtained both in the traditional Calphad approach and using the CSA to describe all the fcc related phases.

We successfully extended the CSA to calculate phase diagrams beyond binaries first to a prototype ternary, next to Ni-Al-Cr, and lastly quaternary Ni-Al-Cr-Re. The CSA

calculated phase diagrams are in accord with available data. Moreover, few parameters are needed when compared with previous descriptions using the point approximation. In addition, the CSA-calculated metastable fcc phase diagrams and the fcc + liquid phase diagrams are what one expects. We also demonstrated that the CSA possesses comparable accuracy when compared with CVM in phase diagram calculation but is computationally much less demanding.

The advantage of computational speed makes CSA a viable model to calculate not only multicomponent phase diagrams but also coherent interphase boundary (IPB) energies. We first demonstrated its suitability for calculating coherent IPB's for prototype ordering and phase-separating alloy systems using the CVM-calculated values as experimental data. We next extended this approach to calculate IPB energies between γ-(Ni) and γ'-(Ni_3Al) in the Ni-Al and (Al) and (Al_3Li) in Al-Li, in accord with the CVM-calculated values and available experimental data within the uncertainties of the measured values. In addition, we also extended the IPB energy calculation to anti-phase boundary (APB) energies in prototype binaries using a similar approach as has been done for IPB energies. These results indicate that one can apply CSA to calculate the coherent γ/γ' IPB and APB energies in multicomponent Ni-based superalloys.

Introduction, Research Objective and Progress

Improvement of future generation turbine engine propulsion systems requires development of better materials that are more durable under the harsh conditions of high temperature and cyclic stress. Traditional development cycles for turbine engine Ni-based superalloys can last more than 10 years. This is partially due to the difficulty of finding an alloy chemistry that provides the desired mechanical properties and material stability. The best way to accelerate the development of new materials is to develop *advanced* computational thermodynamics as an essential tool to provide a blueprint for alloy development and process optimization. Computational thermodynamics enables us to calculate multicomponent phase diagrams that provide the road maps for selecting alloy chemistry and optimizing processing parameters for solidification and heat treatments. The objective of the present study is to adopt the Calphad approach to develop thermodynamic descriptions of Ni alloys containing elements such as Al, Cr, Ru, etc and to simultaneously develop CSA as an enabling model to describe the thermodynamics of the fcc phases such as γ and γ' in Ni-based superalloys.

Phase Diagram calculation and experimental investigation of the Ni-Al-Cr-Ru System

The phase equilibria in the Ni-Al-Ru system have been studied by a number of investigators [80Tsu, 85Cha, 85Pet, 86Cha, 97Har, 97Hor, 97Hor1, 98Hor, 00Hoh]. Most of these investigations have focused on solid-state phase equilibria. The primary phases of solidification reported by Hohls et al. [00Hoh] and Horner et al. [97Hor1] focused on the Al-rich corner whereas the interest here is primarily on the Ni-rich corner. Obtaining a thermodynamic description of this ternary *has been extremely challenging due to the complex phase equilibria and a lack of extensive and internally consistent experimental data.* For the phase equilibrium data, we have relied primarily on the isothermal sections obtained by Chakravorty and West [86Cha] and we did try to use

other earlier published data in our effort to obtain a thermodynamic description but it was impossible to achieve internal consistency. The only enthalpy of formation data available in this system is that of Jung and Kleppa for β-RuAl [92Jun]. This value was adjusted to be more negative since the enthalpy of formation for β-NiAl reported by Nash and Kleppa [01Nas] was less negative than the accepted data reported by Henig and Lukas [75Hen]. We first used the traditional Calphad approach to model this system, i.e., the disordered γ-(Ni) phase and the ordered γ'-$(Ni,Ru)_3Al$ phase were treated as two different phases. During the optimization of model parameters, we found that it was very difficult to maintain the phase relationships at 1273K reported by Chakravorty and West [86Cha]. The γ'-$(Ni,Ru)_3Al$ phase tends to be in equilibrium with the δ-(Ru) phase. In order to achieve equilibrium between β and γ-(Ni), we needed to use a very large negative ternary interaction parameter for the γ-(Ni) phase. Even worse situation was met when we tried to model this system using the more physical realistic CSA model to describe the two fcc-based phases (γ and γ') simultaneously. In this case, the γ'-$(Ni,Ru)_3Al$ phase was always in equilibrium with the δ-(Ru) phase at 1273K no matter how we changed the model parameters. We had every reason to believe that the phase equilibrium data reported in the literature are likely in error.

Experiments were carried out in order to confirm the phase equilibria at 1273K in the Ni-rich corner as well as the primary phases of solidification. Based on the calculated phase diagrams using the preliminarily obtained thermodynamic description, we identified a number of alloy compositions for investigation. The alloy samples were prepared by arc-melting using high purity metals under a partial pressure of argon and then cut into portions. One portion was for investigation in the as-solidified condition. The remaining portion was sealed in quartz tube under a partial pressure of argon for annealing at 1273K for 30 days followed by quenching in water. The as-cast and annealed samples were characterized by XRD, SEM and EPMA. Several annealed samples, in the γ + σ + $β_2$ three-phase region according to Chakravorty and West, show the existence of γ' + σ + $β_2$, *consistent with the CSA calculation but in contradiction with the data of Chakravorty and West.* Fig 1 shows the XRD patterns for the alloy Ni-20Ru-27Al (at.%) after 30-day annealing at 1273K. These data clearly indicate that γ'-$(Ni,Ru)_3Al$ and δ-(Ru) are in equilibrium with each other rather than β and γ-(Ni). In Chakravorty and West's experimental work, the alloys were annealed for only 10 days at 1273K after 10-day annealing at 1523K. At 1523K there are three stable phases in the sample: γ + $β_2$ + σ. When the sample was cooled down to 1273K, the γ phase did not have sufficient time to transform to γ' due to the small driving force from the disordered γ phase to ordered γ' phase. The results we obtained when the samples were annealed for one week at 1273K were the same as those obtained by Chakravorty

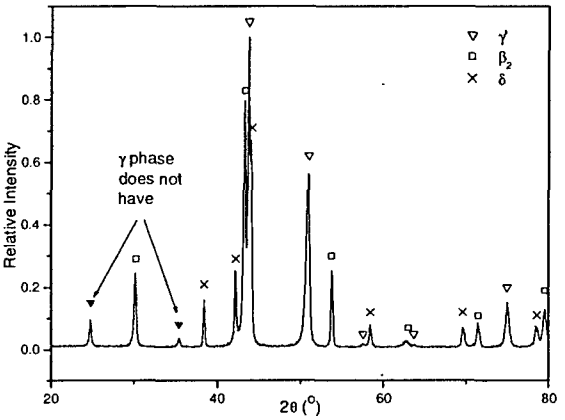

Fig. 1 XRD pattern for alloy Ni-20Ru-27Al (at.%) after 30-day annealing at 1273K

and West, confirming that a longer annealing time is necessary to achieve equilibrium!

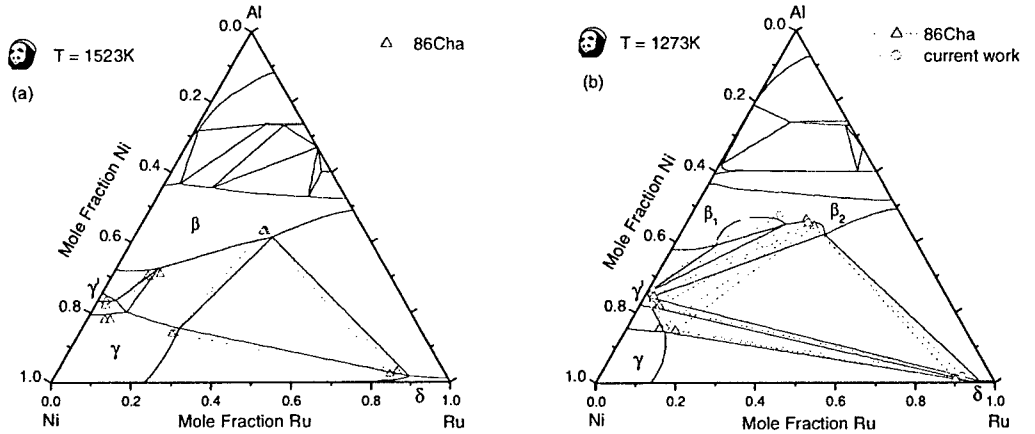

Fig. 2 Comparisons between the CSA-calculated Ni-Al-Ru isothermal sections with experimental data (a) 1523 K (1250°C), and (b) 1273 K (1000°C)

To make a comparison between the calculated results and the available experimental data [86Cha], two isothermal sections were calculated at 1523 and 1273K. As shown in Fig. 2(a), the calculated three-phase equilibria of β + γ-(Ni) + δ-(Ru) and β + γ-(Ni) + γ'-$(Ni,Ru)_3Al$ are in reasonable accord with the measured compositions of the co-existing phases. In the isotherm at 1273K shown in Fig. 2(b), the agreement between calculated

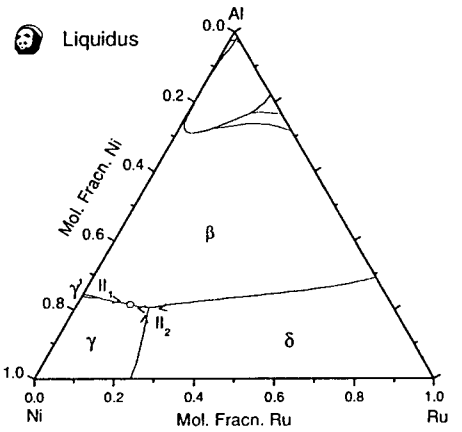

Fig 3. Model-calculated liquidus projection of Ni-Al -Ru ternary system

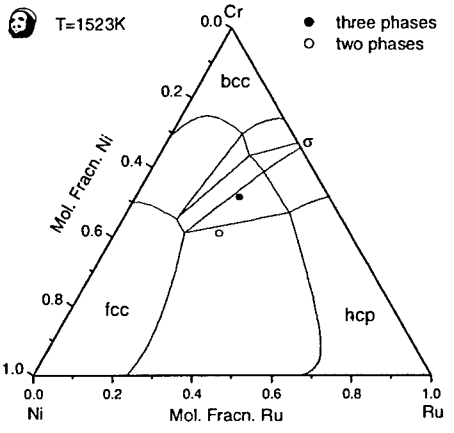

Fig 4. Comparison of calculated Ni-Cr-Ru 1250 °C isotherm with experimental data [85Cha]

and our own experimental results is comparable. As shown in Fig. 3, the calculated liquidus projection shows a large composition region where the primary phase of solidification is β, due to its rather high melting point. Below 50 at% Al, there is a saddle point in the calculated liquidus, i.e. a critical tie line of L + α + γ at this temperature. In addition there exist two type II four-phase invariant equilibria: II_1 (L + γ' = β + γ) at 1592K and 4 at% Ru, and II_2 (L + δ = β + γ) at 1575K and 61 at% Ni, 21 at% Al, respectively. Above 50 at% Al, there is a cascade of invariant equilibria towards the Al-

rich corner with decreases in temperature.

The phase equilibria in Ni-Cr-Ru ternary are much simpler. Figure 4 shows a model-calculated 1250°C isotherm of Ni-Cr-Ru. It is in agreement with the data of [85Cha]. The Al-Cr-Ru ternary is far away from the Ni corner, so a thermodynamic description of this ternary was obtained by extrapolation from the three constituent binaries.

The thermodynamic description of the Ni-Al-Cr-Ru system was obtained from those of the constituent binary and ternaries by extrapolation. As shown in Fig. 5, the calculated isothermal sections with 75 at. % of Ni are in good agreement with the experimental data [85Cha1]. This quaternary description takes into account the experimental data which are judged to be reliable and is believed to offer an understanding of the phase stability in the Ni-rich corner and a useful guide for further experimental investigation in other compositional regions.

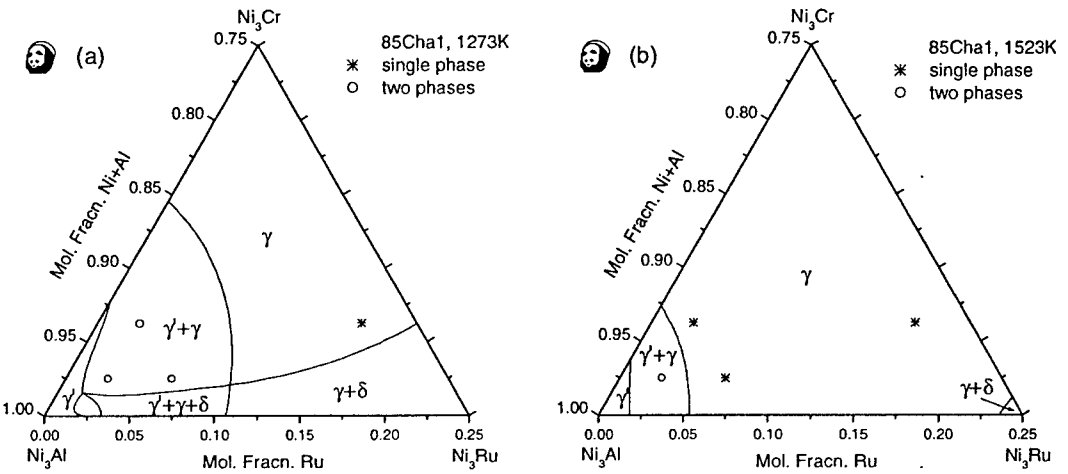

Fig 5. CSA-calculated isothermal sections with 75 at.% of Ni with experimental data[85Cha1] (a) 1273K and (b) 1523K

Phase diagram Calculation – Cluster/Site Approximation

The Cluster/Site Approximation (CSA) takes into account short-range order (SRO), which is essential to satisfactorily describe the thermodynamics of order/disorder transitions such as the transition from γ-(*fcc*) to γ'-($L1_2$) in multicomponent Ni-based superalloys. $L1_2$ is an ordered form of the fcc structure. As noted earlier CSA offers computational advantages over the Cluster Variation Method (CVM) while retains comparable accuracy when compared with CVM-calculated phase diagrams. This makes the CSA a practical model for calculating phase diagrams of real multicomponent alloy systems. We first demonstrated the suitability of CSA in calculating prototype binary phase diagram using CVM-calculated diagrams as the reference [99Oat, 01Zha, 04Cha] and then extended this approach to calculate the technologically important binary Ni-Al phase diagram [03Zha, 04Cha].

In addition, we have successfully extended this approach to calculate the phase diagrams of the prototype coherent ternary Cu-Ag-Au system [2005Cao], again using the CVM-calculated diagrams as the reference [80Kik]. Good agreement was again achieved. However, it is noteworthy to point out that the CSA-calculated isotherm at 240°C as shown in Fig. 6(b) differs from that calculated with CVM shown in fig. 6(a). Figure 6 (b) does not show the existence of the $L1_2$ phase in the Au-rich corner. Prof. C. Colinet of LTPCM-ENSEEG, Saint Martin d'Heres, France subsequently re-calculated this isotherm using the CVM and indeed found the existence of the $L1_2$ phase in the Au-rich corner. In the original CVM calculation, it was necessary to know the existence of this $L1_2$ phase in the Au-rich corner so as to estimate initial values to calculate the compositional stability of this phase. On the other hand, we use the Pandat software, which is able to automatically find the lowest Gibbs energy and thus obtain the most stable phase automatically [2003Che, 2002Che, 2001Che].

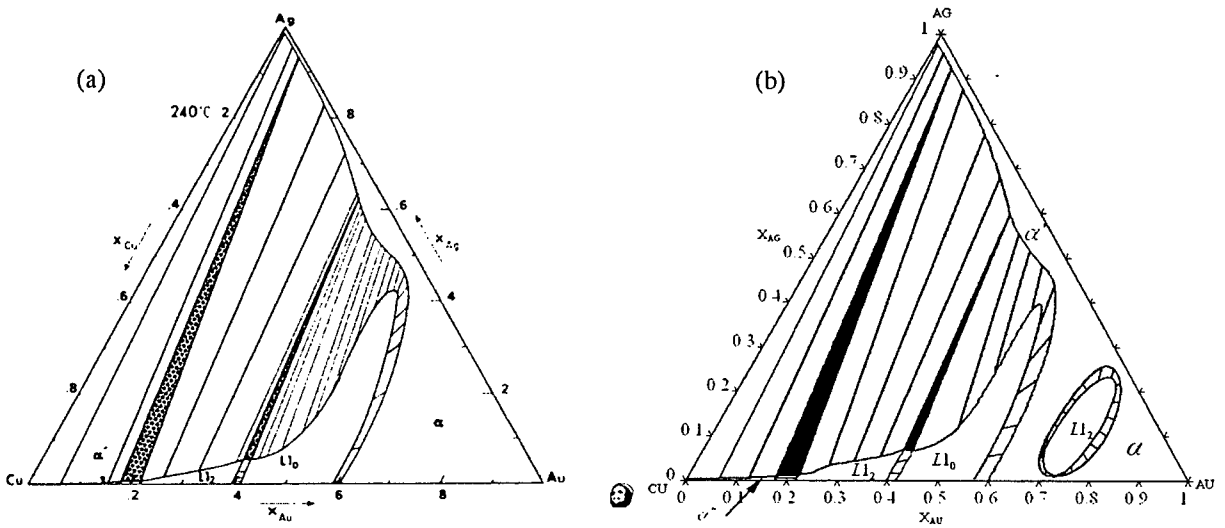

Fig 6. Comparison of prototype Cu-Ag-Au phase diagrams calculated by CVM (a) and CSA (b) at 240 °C

Subsequent to successfully extending the CSA from binaries to calculate prototype coherent phase diagrams of Cu-Ag-Au, we applied this approximation to the fcc phases in the Ni-Al-Cr ternary system. Since the fcc phases in Ni-Al binary had already been modeled using the CSA by Zhang et al. [03Zha], we adopted their description. The model parameters for the fcc phases in the other two constituent binaries were obtained from the experimental data assessed in the literature [05Cao1, 99Hua]. Figures 7(a) and (b) show comparisons between the CSA-calculated isotherm of Ni-Al-Cr at 1273K and the CSA-calculated γ-solvus curves as a function of temperature with experimental data. These γ-solvus curves were calculated at constant values of the mole fraction of Al varying from 0.09 to 0.17. The calculated phase boundaries as shown in Fig. 7(a) are consistent with the experimental data of Ochiai et al. [83Och] and the calculated solvus of the γ-phase shown in Fig. 7(b) is also in accord with the data of Hong et al. [89Hon]. Many other comparisons between calculation and experimentation were made and the agreement is similar to those shown in Fig. 7(a) and (b) but not presented here.

In addition to be able to calculate the stable binary and ternary phase diagrams, it is interesting to use CSA to calculate metastable phase diagrams such as the phase diagrams involving only the fcc phases and only the fcc and liquid phases. For instance the topology of the CSA-calculated metastable binary Ni-Al phase diagram for the fcc-based phase is the same as that calculated using the "first principle" combined with CVM [88Car, 92Pas] to be presented later. On the other hand, Shockley had shown that the calculated phase diagram involving only fcc-based phases based on the point approximation does not have the correct topology [38Sho]. We now present the CSA model, used to calculate the stable 1273 K isotherm shown in Fig: 7(a), to calculate the 1273K isotherm involving only the fcc phases, as shown in Fig. 8(a). As shown in this diagram, the calculated $\gamma + \gamma'$ (or A1 + $L1_2$) phase equilibria in the Ni-rich corner are nearly the same as anticipated since they correspond to the stable equilibria as can be seen from Fig. 7(a). Moreover, the calculated metastable phase equilibria away from the stable region, although different in these two diagrams, are consistent with the phase rule. In other words, the extensions of the phase boundaries to the metastable region show the

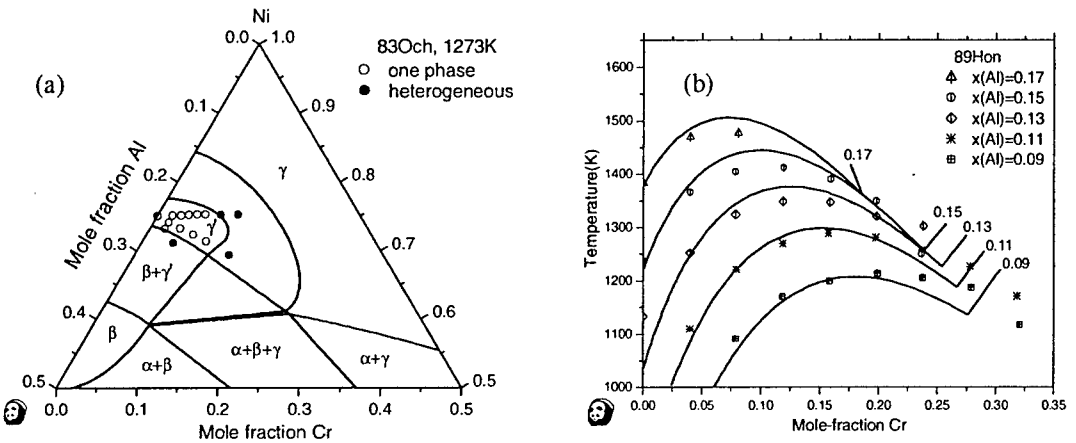

Figure 7. Comparison of calculation with experimental data of Ni-Al-Cr ternary system (a) 1273K (1000°C) isothermal section and (b) the γ-solvus at constant values of Al

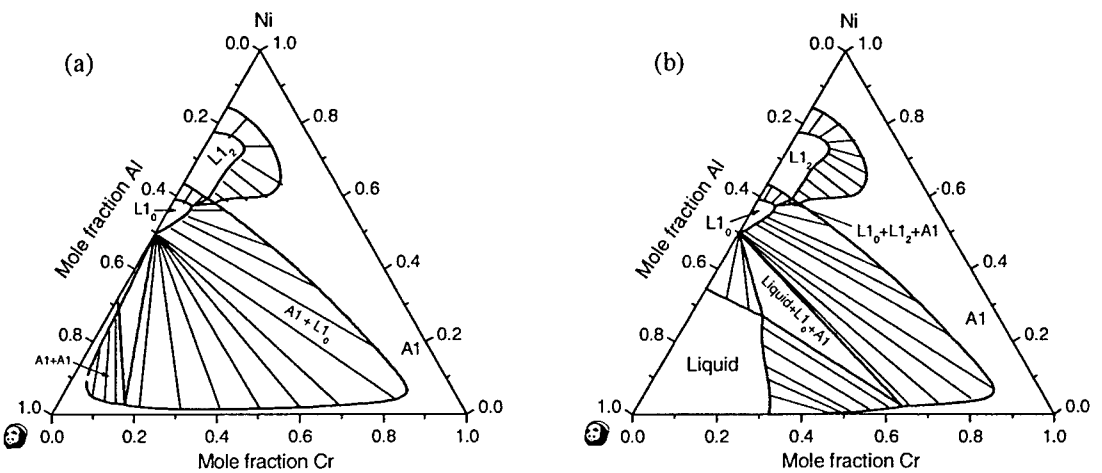

Figure 8. Calculated metastable isotherms at 1273K (1000°C): (a) Phase equilibria involving only the fcc phases and (b) Phase equilibria involving only the fcc and the liquid phases.

existence of two-phase fields of $L1_2$ + $L1_0$, A1 + $L1_0$ as well as a miscibility of the A1 phase with the corresponding three-phase field toward the Al-rich corner. For Fig. 8(b), the liquid phase appears in the Al-rich corner with corresponding two- and three-phase fields involving the liquid phase.

It is worth noting that Zhang et al. [2003Zha] had shown a miscibility gap occurring in the A1 phase in the Al-rich side of the calculated metastable fcc Al-Ni binary diagram as shown in Fig. 9(a). To the best of our knowledge none of the descriptions of Ni-Al obtained from the Calphad approach so far is able to do so [2003Zha, 2004Cha]. We present this binary metastable phase diagram of Ni-Al at this point because we wish to present an isopleth of Ni-Al-Cr at a constant value of 2 at% Cr shown in Fig. 9(b) [2001Cao1] and make a comparison of these two diagrams. Figure 9(a) shows that the

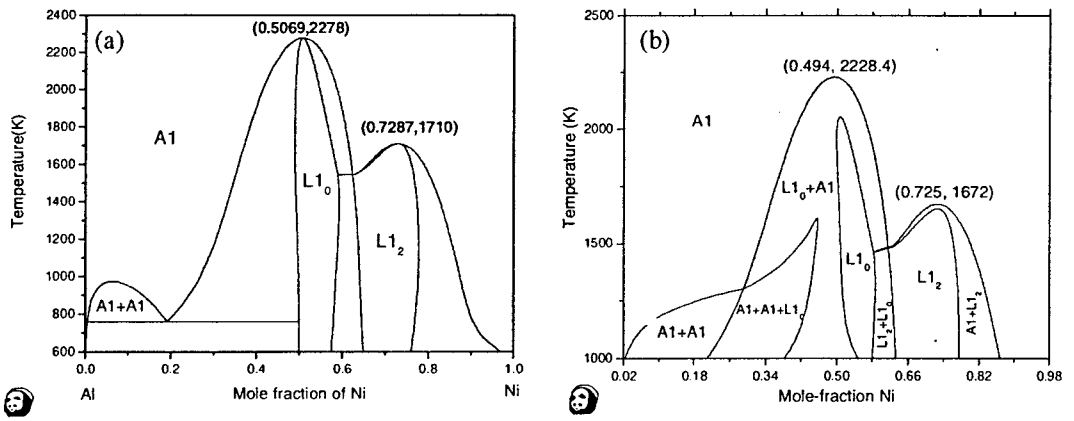

Figure 9 CSA-calculated metastable fcc(A1) phase diagrams: (a) Binary Ni-Al [2003Zha] and (b) An isopleth of Ni-Al-Cr with constant value of 2 at % Cr [2005Cao1]

A1(fcc) phase is stable at high temperatures. With decreasing temperature, the $L1_0$ appears at 50 at% Ni, the $L1_2$ phase at 75 at% Ni, and two A1 (fcc) phases toward the Al-rich side. The calculated isopleth of Ni-Al-Cr with 2 at% Cr has similar features except (i) a three-phase field of A1 + A1 + $L1_0$ appears between the 2 two-phase fields of A1 + A1 and A1 + $L1_0$ and (ii) both the $L1_0$ and $L1_2$ phases no longer melt congruently as should be the case. These results are expected since a binary invariant such as the binary monotectoid, A1 + A1 + $L1_0$, becomes a tie-triangle in the ternary region over a range of temperatures. Of course there is also another three-phase equilibrium of A1 + $L1_0$ + $L1_2$ also shown in this diagram at ~ 1470K and ~ 60 at% Ni. Many other diagrams could be calculated such as the liquidus projection of the metastable phase diagram involving only the fcc (A1) and liquid phases. Additional metastable diagrams were presented elsewhere [05Cao1] and are not repeated here.

We have successfully using CSA to calculate the quaternary Ni-Al-Cr-Re system. The preliminary results presented in Figs. 10(a) and (b) show excellent agreement between calculation and experimentation is achieved.

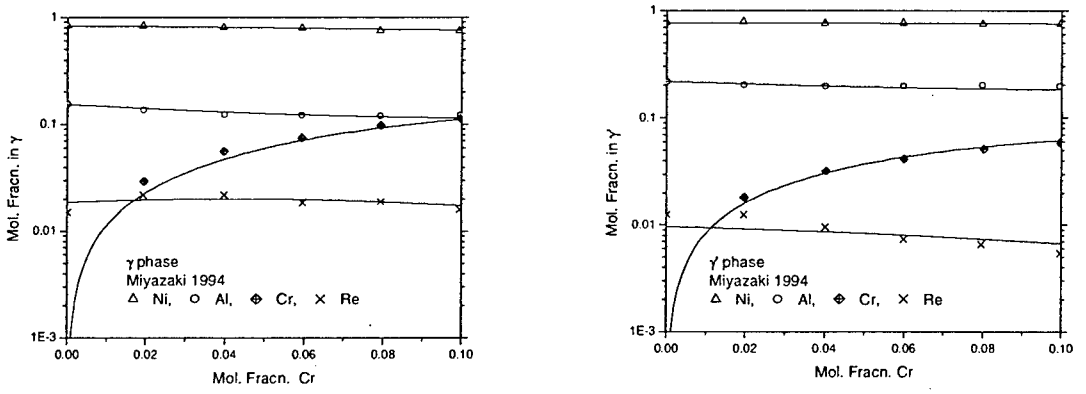

Fig 10. The CSA-calculated compositions of (a) γ and (b) γ' of the Ni-Al-Cr-Re alloys with 1.5 at% Re and x_{Ni}-x_{Al} = 0.625 at 1313K.

Interphase Boundary (IPB) Energy Calculation using CSA

In view of the relative computational simplicity of the CSA and the fact that it is able to calculate phase diagrams of binary and higher order alloys system, we have been first exploring the use of the CSA to calculate coherent IPB energies for the fcc/$L1_2$ phases. Our motivation was: if this approach were shown to be a suitable one, we could then extend the use of this approach to calculate IPB energies, for instance, between γ and γ' first in binary Ni-Al and then in multicomponent Ni-based superalloys. These quantities are urgently needed for describing microstructure evolution when an alloy undergoes thermal treatment using kinetic modeling such as the phase-field approach. We first used the CSA to calculate the IPB energies of binary immiscible alloys and then those between the prototype fcc-(Cu, Au) and the ordered $L1_2$-(Cu_3Au) phases. The calculated results for the immiscible binary case agree with those obtained by Kikuch and Chen [95Kik] using the CVM but deviate from those obtained by Lee and Aaronson [80Lee] using a regular solution model. The results have been presented elsewhere and repeated here [2005Cao2].

Comparisons of the CSA-calculated coherent IPB energies between the fcc-(Cu, Au) and the $L1_2$-(Cu_3Au) phases with the CVM-calculated values [79Kik] are presented in Figs. 11(a) and (b). In both cases the tetrahedron approximation was used. Our calculation was carried out following the approach of Kikuchi and Cahn but using the CSA instead of the CVM. The pair exchange energy W for the CSA calculation was taken from Oates et al. [99Oat]. As shown in Fig. 11(b) the CSA-calculated IPB energies for the (100) plane are in accord with those given in Fig. 11(a) calculated by Kikuchi and Cahn from the congruent point down to low temperatures. As also shown in Fig. 12(b), the CSA-calculated concentration profile for the (100) IPB between these two phases at the congruent point are also in accord with the CVM-calculated values shown in Fig. 12(a). These results led us to believe that the CSA could be used to calculate IPB energies and should be explored further.

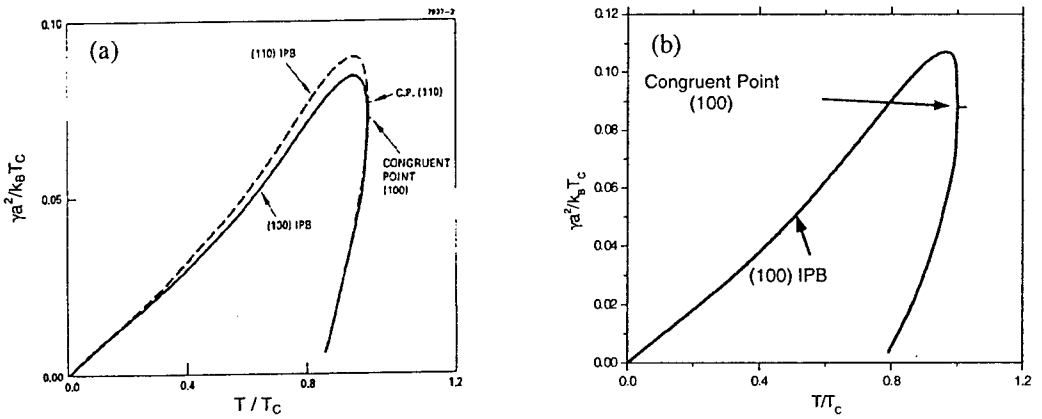

Figure 11 Calculated coherent IPB energies of the fcc-(Cu, Au) and $L1_2$-Cu_3Au phases using the tetrahedron approximation: (a) CVM-Calculation for the (100) & (110) planes, (b) CSA calculation for (100) planes.

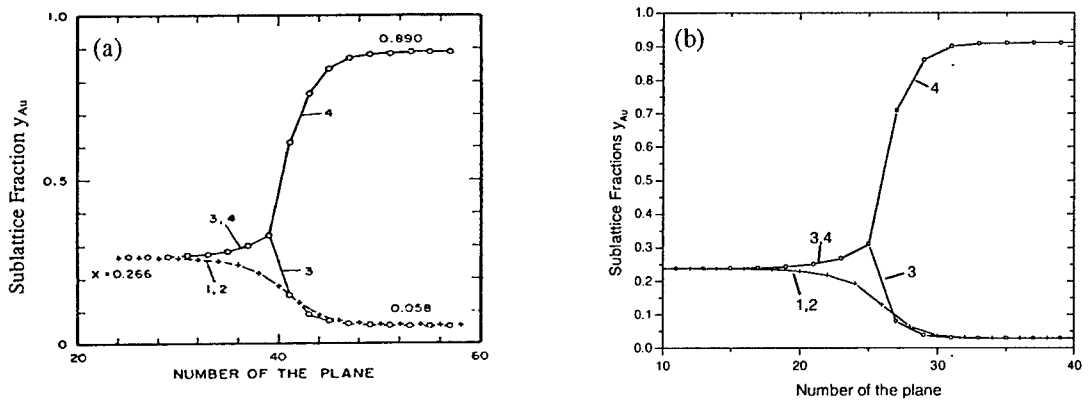

Figure 12 Calculated concentration profile for the (100) IPB at the congruent point: (a) CVM and (b) CSA.

As noted previously [79Kik, 96Ast1], the vanishing of the calculated IPB energy at 0K using the tetrahedron approximation is due to the neglect of the longer-range interaction in the lattice. Using the tetrahedron-octahedron approximation of the CVM (TO-CVM), expressed in terms of the parameter $\alpha = W_2/W_1$ for α = -0.1 and -1.0, Asta [96Ast1] calculated the phase diagrams of the prototype Cu-Au binary and then the coherent IPB energies between the fcc-(Cu,Au) and the $L1_2$-(Cu_3Au) phases. The terms W_2 and W_1 denote the next nearest neighbor and the nearest neighbor pair exchange energies, respectively. Figures 13(a) and (b) show the TO-CVM and TP-CSA calculated phase diagram and coherent IPB energies between the fcc-(Cu, Au) and $L1_2$-Cu_3Au phases for the (100) planes. The TO-CVM calculated values were taken from Asta [96Ast1] and shown in these figures as discrete points. As shown in Fig. 13(b) the coherent IPB energy at 0K is finite and decreases first with increasing temperature and then change slowly with further increases in temperatures. We used the tetrahedron-pair approximation of the CSA (TP-CSA) to calculate the phase diagram and coherent IPB

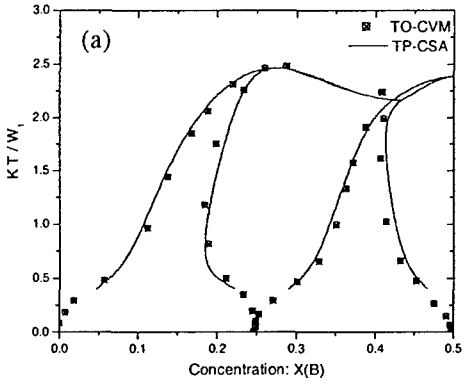

Figure 13 (a) Calculated prototype Cu-Au phase diagram with $\alpha = -0.1$ with the TO-CVM calculated values shown as discrete points [96Ast1] and the TP-CSA values as smoothed

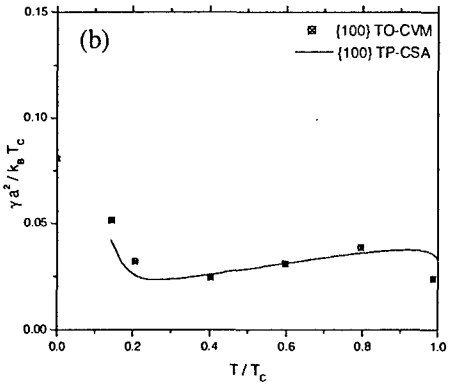

Figure 13 (b) Calculated IPB energies between the fcc and $L1_2$ phases with $\alpha = -0.1$. The TO-CVM calculated values are shown as discrete points [96Ast1] and TP-CSA values as a smoothed curve.

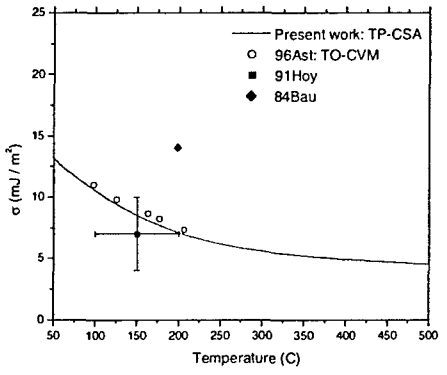

Figure 14 (a) Comparisons of TP-CSA-calculated coherent IPB energies between fcc-(Al) and $L1_2$-Al_3Li with the TO-CVM values and the experimental data [91Hoy, 84Bau].

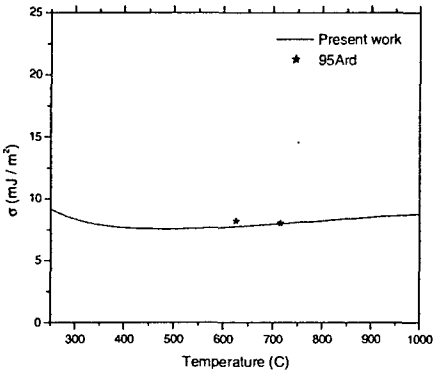

Figure 14 (b) Comparisons of TP-CSA-calculated coherent IPB energies between γ and γ' in Ni-Al with experimental data [90Mar, 95Ard].

energies [99Vak, 06Cao]. Our TP-CSA calculated reduced temperatures expressed as a function of composition as shown in Fig. 13(a) represented by smoothed curves are in accord with the TO-CVM calculated values. Likewise, the TP-CSA calculated coherent IPB energies given in Fig. 13(b) shown as a smoothed curve is in accord with the TO-CVM calculated results. We did not calculate the values down to 0K due to numerical difficulties, which will be resolved in the near future. Nevertheless, the fact that the calculated values are in reasonable accord with the TO-CVM calculated results [96Ast1] is encouraging.

We next extended the TP-CSA to calculate the coherent IPB energies between the fcc and $L1_2$ phases in two real alloy systems, i.e. Al-Al_3Li and Ni-Al. As shown in Fig. 14(a) the TP-CSA calculated IPB energies are in accord with the TO-CVM calculated values [96Ast]. Within the uncertainties of the measurements, there is agreement between the calculated values and the experimental data of Hoyt and Spooner [91Hoy] and Baumann and Williams [84Bau]. Figure 14(b) shows that the TP-CSA calculated IPB energies

between γ and γ' in Ni-Al are in accord with the experimental values of Ardell [95Ard]. Ardell re-evaluated the data of Marsh and Chen [90Mar] and obtained values in the range of 2 mJ/m^2 but not shown in this figure. It is worth noting that Dr. Chris Woodward of the AFML, Dayton, OH [2004Woo] shared his calculation of IPB energies between γ and γ' in Ni-Al with us. He used a "first principles" cluster expansion method coupled with Monte Carlo calculations to estimate the interfacial width and excess free energy in γ and γ' in Ni-Al. For temperatures in the range of experimental measurements (see Figure 14(b)) his calculated IPB energies are in good agreement with our estimates, and with the available results from experimental measurements. The concentration profile across a coherent (100) γ/γ' interface obtained from recent grand-canonical Monte Carlo simulations at 700K [04Mis] is shown in Figure 15(a). The concentration profile obtained from the current study using the TP-CSA is also plotted in Figure 15(b) for comparison. As pointed out by Mishin [04Mis], the long-range order does not drop to zero abruptly at the interface plane but rather decays gradually over 4 - 6 (2 0 0) atom layers around the interface, as does also the average Al concentration. The comparison in Figures 15(a) and (b) shows that the TP-CSA predicts a very similar interfacial width with the one derived from the Monte Carlo calculations, although there is a small difference in the average Al concentrations for the bulk γ and γ' phases, which is due to the fact that the bulk phase diagram determined by these two methods are slight different from one another. All these results indicate that the CSA, computationally less demanding than the CVM, offers an alternative and perhaps practical approach to calculate (or estimate) coherent IPB energies for γ and γ' in other Ni binaries and even to higher order alloys of practical importance.

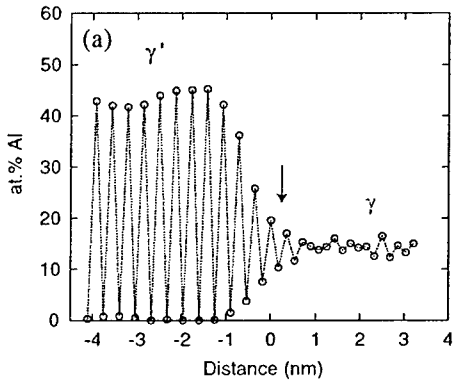

Figure 15 (a) Concentration profile across the coherent (1 0 0) γ/γ' interface obtained by grand-canonical Monte Carlo simulations at 700 K. The points represent Al concentration in individual (2 0 0) layers parallel to the interface. The arrow marks the initial position of the interface at 0K [04Mis].

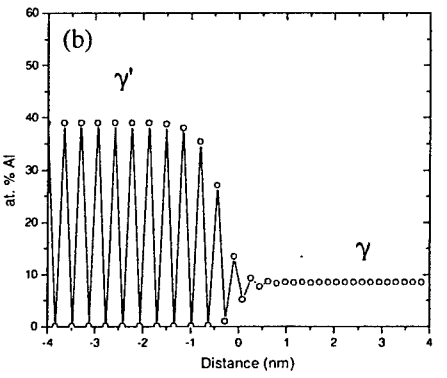

Figure 15 (b) Concentration profile across the coherent (1 0 0) γ/γ' interface obtained from the present study using the TP-CSA.

Anti-phase Boundary (APB) Energy Calculation – Cluster/Site Approximation

After extending the CSA to multicomponent systems and using the CSA to calculate IPB energies, we use the CSA to calculate anti-phase boundary (APB) energies in Cu-Au binary using a similar approach as has been done for IPB energies. Fig. 16 shows the CSA-calculated (solid line) and the CVM-calculated (scattered points) {100} APB energies as a function of temperature with the composition of Au, x(Au) = 0.267. Both results indicate an identical trend and predict a maximum in σ. The CSA-calculated value of $\sigma a^2/K_BT_C$ at the congruent point is around 0.2 for the (100) APB and 0.1 for the (100) IPB. This agrees with the relation between σ_{APB} and σ_{IPB} for (h, k, 0) orientations at the congruent point given by Kikuchi and Cahn [79Kik], i. e. $\sigma_{APB} = 2\sigma_{IPB}$. Thus the (100) APB could either consist of two (100) IPB's with a disordered layer in between or it coincidently has the same free energy. Fig. 17(a) and 17(b) show the calculated profiles of the APB and IPB and conform that the disordered layer is part of the APB and that indeed the APB has become two IPB's. As the temperature decreases from the congruent point to $T/T_C = 0.9$, the APB narrows but the internal structure of the APB remains the same as shown in Fig. 17(a). However, according to our CSA-calculated results, there is a structure change when temperature decreases to $T/T_C = 0.83$. This is also in accord with those results obtained from the CVM [79Kik]. But the CSA calculation is computational much less demanding.

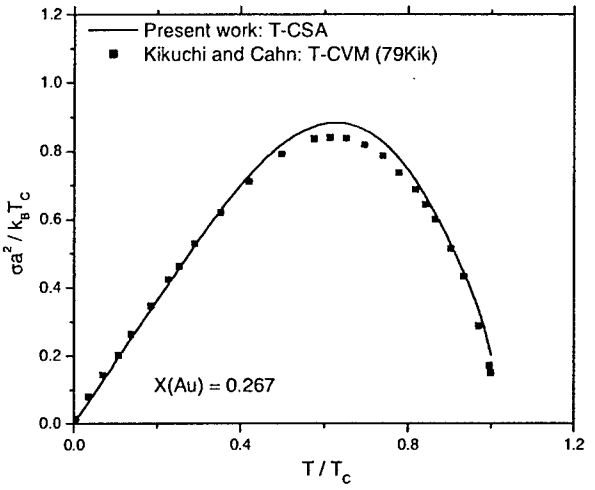

Figure 16. Comparison of (100) APB energies as a function of temperature at the constant composition x(Au) = 0.267 calculated by CVM and CSA

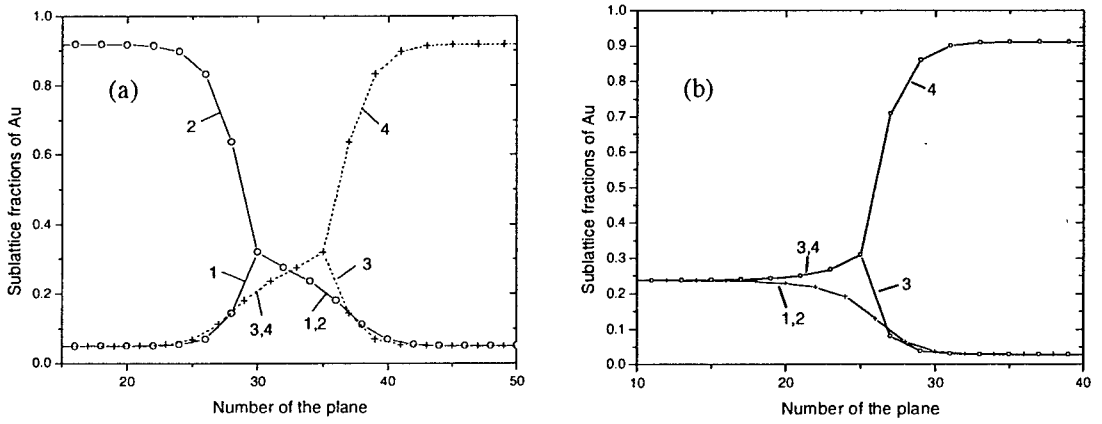

Figure 17. The calculated profiles of the (100) APB (a) and IPB (b) at the congruent point.

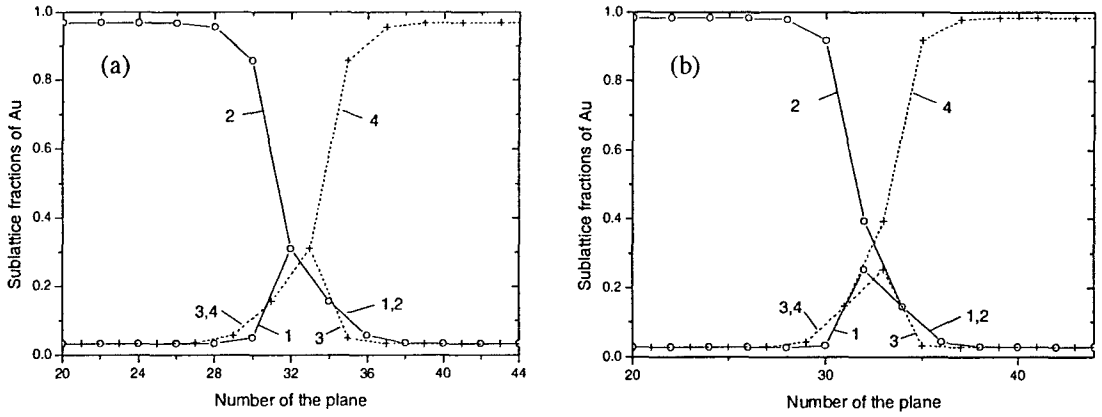

Figure 18. There is a structural change in the core of (100) APB's between $T / T_C = 0.9$ (a) and 0.83 (b).

Acknowledgement

This work was sponsored by the Air Force Office of Scientific Research (AFOSR), USAF, under grant/contract number F49620-03-1-0083. The views and conclusions contained herein are those of the authors and should not be interpreted as necessarily representing the official policies or endorsements, either expressed or implied, of the AFOSR or the U. S. Government.

Personnel Supported

Jun Zhu	Graduate Student, UW-Madison.
Weisheng Cao	Graduate Student, UW-Madison.
Y. Austin Chang	Wisconsin Distinguished Professor, UW-Madison.

Publications and Presentations

1) Y. A. Chang, S.-L. Chen, F. Zhang, X.-Y. Yan, F.-Y. Xie , R. Schmid-Fetzer, and W. A. Oates, "Phase Diagram Calculation: Past, Present and Future", Prog. Mater. Science, 2004, 49, 313-345.

2) Y. A. Chang, "Application of the Cluster/Site Approximation to the Calculation of Multicomponent Alloy Phase Diagrams", presented at the International Conference CALCON 2004, Santa Fe, NM, USA, 6/29/04.

3) W. Cao, J. Zhu, S.-L. Chen, W. A. Oates, and Y. A. Chang, "Application of the Cluster/Site Approximation to the Calculation of Multicomponent Alloy Phase Diagrams", presented at the International Conference, Calphad XXXIII, Krakow, Poland, 05/31/04.

4) W. Cao, Y. A. Chang, J. Zhu, S.-L. Chen and W. A. Oates, "Application of the Cluster/Site Approximation to the Calculation of Multicomponent Alloy Phase Diagrams", Acta Mater., 2005, 53, 331-335.

5) W. Cao, J. Zhu, Y. Yang, F. Zhang, S.-L. Chen, W. A. Oates and Y. A. Chang, "Application of the Cluster/Site Approximation to fcc Phases in Ni-Al-Cr", Acta Mater., 2005, 53, 4189-4197.

6) W. Cao, Y. A. Chang, J. Zhu, S.-L. Chen and W. A. Oates, "Application of the Cluster/Site Approximation to the Calculation of Multicomponent Alloy Phase Diagrams", Acta Mater., 2006, 54, 377-383. Presented at the TMS 2005, San Francisco, CA, USA, 02/16/05. (*Presented by W. Cao*).

7) W. Cao, J. Zhu, F. Zhang, W. A. Oates, M. Asta and Y. A. Chang, "Application of the Cluster/Site Approximation to the Calculation of Coherent Inter-phase Boundary Energy", presented at the TMS 2005, San Francisco, CA, USA, 02/15/05. (*Presented by W. Cao*).

8) W. Cao, J. Zhu, Y. Yang, W. A. Oates and Y. A. Chang, "Thermodynamic Stability of Co/Cu Multilayered Nanostructures", Script Mater., 2005, 53, 1379-1382.

9) W. Cao, J. Zhu, F. Zhang, W. A. Oates, M. Asta and Y. A. Chang, "Application of the Cluster/Site Approximation to the Calculation of Coherent Inter-phase Boundary Energy", Acta Mater., 2006, 54, 377-383.

10) Y. A. Chang, "Phase Diagram Calculation in Teaching, Research and Industry", Metall. Mater. Trans., 2006, 37A, 273-305. Also Metall. Mater. Trans., 2006, 37B, 7-39.

11) W. Cao, J. Zhu, and Y. A. Chang, "Application of the CSA to FCC Phases in Calculating Multi-Component Nickel-Based Alloys", Poster Session 2: Vapor Deposited Materials/High Temperature Chemistry and Materials Properties/Oxidation and Corrosion at the Gordon Conference on High Temperature Materials, Processes, and Diagnostics 2006, Colby college, ME, USA, 07/19/06. (Presented by W. Cao).

12) J. Zhu, W. Cao, Y. Yang and Y. A. Chang, "Thermodynamic modeling and experimental investigation of the Ni-rich region of the Ni-Al-Ru System", Poster Session 2: Vapor Deposited Materials/High Temperature Chemistry and Materials Properties/Oxidation and Corrosion at the Gordon Conference on High Temperature Materials, Processes, and Diagnostics 2006, Colby college, ME, USA, 07/19/06. (Presented by J. Zhu).

Honors and awards

1) Best poster of Poster Session 2: Vapor Deposited Materials/High Temperature Chemistry and Materials Properties/Oxidation and Corrosion at the Gordon Conference on High Temperature Materials, Processes, and Diagnostics 2006, Colby college, ME, USA, 07/19/06. ("Application of the CSA to FCC Phases in Calculating Multi-Component Nickel-Based Alloys", Presented by W. Cao).

The following four have been awarded to Y. Austin Chang

2) The 2005 Distinguished Award, International Workshop on Advanced Intermetallic and Metallic Materials.

3) Wisconsin Idea Fellow, University of Wisconsin System, 2004-2005.

4) Distinguished Speaker, Department of Materials Science & Engineering, Penn State University, 2004.

5) Identified as a highly cited materials scientists by ISIHighlyCited, 2003, covering the period 1981-1999.

6) Edward DeMille Campbell Memorial Lecturer Award, ASM-International, 2003.

References

[38Sho] W. Shockley, J. Chem. Phys., 1938, 6, 130-44.

[51Kik] R. Kikuchi, Phys. Rev., 1951, 81, 988.

[61Rau] Raub, E.; Z. Metallkd., 1961, 52, 831-833.

[64Kor] Kornilov, I.I.; Izv. Akad. Nauk SSSR, Met. Govn. Delo, 1964, 4, 159-165.

[75Hen] E. T. Henig and H. L. Lukas, Z. Metallkd., 1975, 66, 98-106.

[79Def] D. de Fontaine, "Configurational Thermodynamics of Solid Solutions" in Solid State Physics (Academic Press, New York, 1979) 34, 73.

[79Kik] R. Kikuchi, and J. W. Cahn, Acta Metall., 1979, 27, 1337.

[80Kik] R. Kikuchi, J.M. Sanchez, D. deFontaine, and H. Yamauchi, Acta Metall., 1980, 28, 651.

[80Tsu] V.F. Tsurikov, E.M. Sokolovskaya, and E.F. Kazakova, *Vestnik Moskovskogo Universiteta, Seriya 2: Khimiya* (1980), **21**(5), 512-14.

[83Och] S. Ochiai, Y. Oya, T. Suzuki, Bull P M E (T I T) 1983, 52,1.

[84Bau] S. F. Baumann and D. B. Williams, Scripta metall. 1984, 18, 611.

[85Cha] S. Chakravorty and D. R. F. West, Scripta metall. 1985, 19, 1355-60.

[85Cha1] S. Chakravorty, H. Hashim and D. R. F. West, J. Mater. Sci. 1985, 20, 2313-22.

[85Pet] L.A. Petrovoj, in N.V. Ageeva, (ed.), *Diagrammy Sostoyaniya Metallicheskikh Sistem, Viniti, Moscow*, 30, 1985, 323.

[86Cha] S. Chakravorty and D. R. F. West, J. Mater Sci., 1986, 21, 2721.

[88Ard] A. J. Ardell. Phase Transformations 87 (edited by G. W. Lorimer). Institute of Metals. London (1988)

[88Ans] S. M. Anlage et al, J. Less-Common Met, 1988, 136, 237.

[88Car] Carlsson AE, Sanchez JM. Solid State Commun 1988; 65:527.

[89Hon] Y. M. Hong, H. Nakayima, Y, Mishima, and T. Suzuki, ISIJ International, 1989, 29, 78.

[90Mar] C. Marsh and Haydn Chen, Acta Metall. Mater., 1990, 38 2287.

[91Hoy] J. J. Hoyt and S. Spooner, Acta Metall. 1991, 39, 689.

[92Jun] W.-G. Jung, O. J. Kleppa, Metall. Trans., 1992, 23B, 53-56.

[92Lee] B. J. Lee, CALPHAD, 1992, 16, 121-149.

[92Pas] Pasturel A, Colinet C, Paxton AT, van Schilfgaarde M. J Phys Condens Matter 1992; 4:945.

[94Def] D. De Fontaine, "Cluster Approach to Order-Disorder Transformations in Alloys", Solid State Physics, Vol. 47, H. Ehrenreich and D.Turnbull, eds, Academic Press, 1994. pp. 33-176.

[95Ard] Alan J. Ardell, Interface Science, 1995, 3 119.
[96Ast] M. Asta, Acta mater. 1996, Vol. 44, No. 10,4131-4136.
[97Har] A.S. Harte, P.M. Hung, I.J. Horner, et. al. Advances in X-Ray Analysis, 1997, 39, 747-753.
[97Hor] I.J. Horner, L.A. Cornish, and M.J. Witcomb, J. Alloys and Comp., 1997, 256, 213-220.
[97Hor1] I.J. Horner, L.A. Cornish, and M.J. Witcomb, J. Alloys and Comp., 1997, 256, 221-227.
[98Maz] Mazhuga, T.G. et al; CALPHAD, 1998, 22, 59-67.
[98Hor] I.J. Horner, N. Hall, L.A. Cornish, et.al., *J. Alloys and Comp.*, 1998, 264, 173-179.
[99Dan] Danilenko, V.M. et al; Powder Metallurgy and Metal Ceramics, Vol. 38 Nos. 5-6 (1999) 254-260.
[99Hua] W. Huang and Y. A. Chang, Intermetallics, 1998, 6, 487-498; Corrigendum: Intermetallics, 1999, 7, 625-626.
[99Oat] W. A. Oates, F. Zhang, S.-L. Chen and Y. A. Chang, Phys. Rev. B, 1999, 59, 11221-11225.
[00Hoh] J. Hohls, L.A. Cornish, P. Ellis, and M.J. Witcomb, J. Alloys and Comp., 2000, 308, 205-215.
[01Nas] P. Nash and O. J. Kleppa, J. Alloys Comp., 2001, 321, 228.
[01Zha] J. Zhang, W. A. Oates, F. Zhang, S.-L. Chen, K.-C. Chou and Y, A. Chang, Intermetallics, 2001, 9, 5-8.
[03Col] Prof. Catherine Colinet of the university of Grenoble, France, did the calculation to show that indeed the $L1_2$ is stable in the fcc Au-rich regime of Cu-Ag-Au.
[03Zha] F. Zhang, Y. Du, W. A. Oates, S.-L. Chen, and Y. A. Chang, Acta Mater, 2003, 51, 207-216.
[04Cha] Y. A. Chang, S.-L. Chen, F. Zhang, X.-Y. Yan, F.-Y. Xie , R. Schmid-Fetzer, and W. A. Oates, Prog. Mater. Science, 2004, 49, 313-345.
[04Mis] Y. Mishin, Acta Mat., 2004, 52, 1451.
[04Pol] T. Pollock, University of Michigan, Ann Arbor, MI, 2004, private communication.
[05Cao] W. Cao, Y. A. Chang, J. Zhu, S.-L. Chen and W. A. Oates, Acta Mater., 2005, 53, 331-335.
[05Cao1] W. Cao, J. Zhu, Y. Yang, F. Zhang, S.-L. Chen, W. A. Oates and Y. A. Chang, Acta Mater., 2005, 53, 4189-4197.
[05Cao2] W. Cao, W. A. Oates and Y. A. Chang, Scripta Mater, 2005, 53, 1379-1382
[06Cao] W. Cao, J. Zhu, F. Zhang, W. A. Oates, M. Asta and Y. A. Chang, Acta Mater., 2006, 54, 377-383.